Dimetallacycles from Monomeric 18-Electron $M(CO)_4(\eta^1\text{-}C_2H_2)$ and $M(CO)_5$ (M = Ru, Os) Building Blocks: Synthesis and Mechanism of Formation

Gong-Yu Kiel, Zhongsheng Zhang, J. Takats, and R. B. Jordan*

Department of Chemistry, University of Alberta, Edmonton, Alberta, Canada, T6G 2G2

Received January 21, 2000

The synthesis and spectroscopic characteristics of $M(CO)_4(\eta^2\text{-}C_2H_2)$ (M = Os, **1a**; Ru, **1b**) are presented. The compounds readily react with the parent pentacarbonyls to yield the dimetallacyclic compounds $Os_2(CO)_8(\mu\text{-}C_2H_2)$ (**2**) and $MRu(CO)_8(\mu\text{-}C_2H_2CO)$ (M = Os, **3**; Ru, **4**). The structure of the compounds, based on IR and ^{13}C NMR spectroscopies, including extensive ^{13}C labeling, depends on the $M(CO)_5$. Kinetic studies of the formation of **2** and **3** show that, in both cases, the reaction is slowed by the addition of free CO, but the inhibition is much greater with $Os(CO)_5$. The initial step is dissociation of CO from $Os(CO)_4(\eta^2\text{-}C_2H_2)$, and the inhibition results from the competition between the reverse of this dissociation and reaction of the unsaturated intermediate with $Os(CO)_5$ or $Ru(CO)_5$. With CO added to the system, subsequent steps in the condensation may become rate-limiting. Studies of the $Ru(CO)_5/Os(CO)_4(\eta^2\text{-}C_2H_2)$ system with ^{13}CO-enriched reactants reveal further details about the course of the reaction.

Introduction

The chemistry of metallacyclic and dimetallacyclic compounds[1] continues to be an active area of research in organometallic chemistry. This interest stems from the recognized role such species play in many important reactions[2] and as models for the chemisorption and subsequent transformation of organic substrates on the surface of heterogeneous catalysts.[3] Within this vast domain, alkyne-based dimetallic complexes display a large variety of structural types.[4] The usual synthesis of these compounds starts with a preformed dimetallic precursor;[5] construction from mononuclear building blocks is a rare event.[6] Some time ago we reported the synthesis of $M(CO)_4(\eta^2\text{-alkyne})$ (**1**) compounds[7] (M = Fe, Ru, Os) and disclosed their greatly enhanced reactivity compared to their parent pentacarbonyls, $M(CO)_5$. They undergo much more facile CO exchange and phosphine substitution. This was quantified by a kinetic study[8] that showed that the replacement of CO by phosphines in the hexafluorobutyne (HFB) complexes $M(CO)_4(\eta^2\text{-}C_2(CF_3)_2)$ is faster by factors of 10^{13}, 10^3, and 10^6 for M = Fe, Ru, and Os, respectively. A kinetic study of phosphine substitution (eq 1) on the acetylene complex[9] $Os(CO)_4(\eta^2\text{-}C_2H_2)$ has shown that it is ~10 times more reactive than the HFB complex, with kinetic parameters of $\Delta H^* = 90.7 \pm 1$ kJ mol^{-1}, $\Delta S^* = 30.1 \pm 4$ J mol^{-1} K^{-1}, and $k_1 = 3.0 \times 10^{-2}$ s^{-1} at 25 °C in pentane.

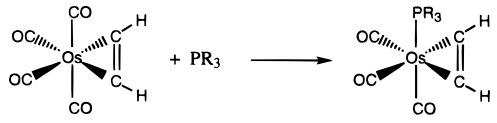

1 (1)

The synthetic studies also have shown that **1** can undergo surprisingly facile reactions with 18-electron group 8, $M(CO)_5$ (M = Ru, Os), and group 9, $Cp'M'(CO)_2$ (M′ = Co, Rh, Ir; Cp′ = η^5-C_5Me_5, η^5-C_5H_5), molecules under mild conditions to form various dimetallacyclic species.[7,10] The reactions of interest here are given by

(1) (a) Lindner, E. *Adv. Heterocycl. Chem.* **1986**, *39*, 237. (b) Chisholm, M. H., Ed. *Polyhedron Symposia in Print No. 5, Polyhedron* **1988**, *7*, 757. (c) Lotz, S.; van Rooyen, P. H.; Meyer, R. *Adv. Organomet. Chem.* **1995**, *37*, 219. (d) El Amouri, H.; Gruselle, M. *Chem. Rev.* **1996**, *96*, 1077.

(2) (a) Collman, J. P.; Hegedus, L. S.; Norton, J. R.; Finke, R. G. *Principles and Applications of Organotransition Metal Chemistry*; University Science Books: Mill Valley, CA, 1987; Chapters 9 and 16. (b) Jennings, P. W.; Johnson, L. L. *Chem. Rev.* **1994**, *94*, 2241.

(3) (a) Sheppard, N. *Annu. Rev. Phys. Chem.* **1988**, *39*, 589. (b) Zaera, F. *Chem. Rev.* **1995**, *95*, 2651.

(4) (a) Hoffman, D. M.; Hoffmann, R.; Fisel, C. R. *J. Am. Chem. Soc.* **1982**, *104*, 3858. (b) Holton, J.; Lappert, M. F.; Pearce, R.; Yarrow, P. I. W. *Chem. Rev.* **1983**, *83*, 135.

(5) For some leading references see: (a) Dickson, R. S. *Polyhedron* **1991**, *10*, 1995. (b) Knox, S. A. R. *J. Organomet. Chem.* **1990**, *400*, 255. (c) Johnson, K. A.; Gladfelter, W. L. *Organometallics* **1992**, *11*, 2534. (d) Adams, R. D. *Chem. Soc. Rev.* **1994**, 335. (e) Wang, L.-S.; Cowie, M. *Can. J. Chem.* **1995**, *73*, 1058. (f) Casey, C. P.; Cariño, R. S.; Hayashi, R. K.; Schladetzky, K. D. *J. Am. Chem. Soc.* **1996**, *118*, 1617.

(6) (a) Beck, W.; Müller, H.-J.; Nagel, U. *Angew. Chem., Int. Ed. Engl.* **1986**, *25*, 734. (b) Davidson, J. L.; Manojlovic-Muir, L.; Muir, K. W.; Keith, A. N. *J. Chem. Soc., Chem. Commun.* **1980**, 749. (c) Koie, Y.; Shinoda, S.; Saito, Y.; Fitzgerald, B. J.; Pierpont, C. *Inorg. Chem.* **1980**, *19*, 770. (d) Davidson, J. L.; Green, M.; Stone, F. G. A.; Welch, A. *J. Chem. Soc., Dalton Trans.* **1979**, 506.

(7) (a) Gagné, M. R.; Takats, J. *Organometallics* **1988**, *7*, 6850. (b) Burn, M. J.; Kiel, G.-Y.; Seils, F.; Takats, J.; Washington, J. *J. Am. Chem. Soc.* **1989**, *111*, 6850. (c) Cooke, J.; Takats, J. *J. Am. Chem. Soc.* **1997**, *119*, 11088.

(8) Pearson, J.; Cooke, J.; Takats, J.; Jordan, R. B. *J. Am. Chem. Soc.* **1998**, *120*, 1434.

(9) Mao, T.; Zhang, Z.; Washington, J.; Takats, J.; Jordan, R. B. *Organometallics* **1999**, *18*, 2331.

(10) Takats, J. *J. Cluster Sci.* **1992**, *3*, 479.

10.1021/om0000515 CCC: $19.00
Publication on Web 06/16/2000

eqs 2 and 3. With $Os(CO)_5$ a CO is lost and the product

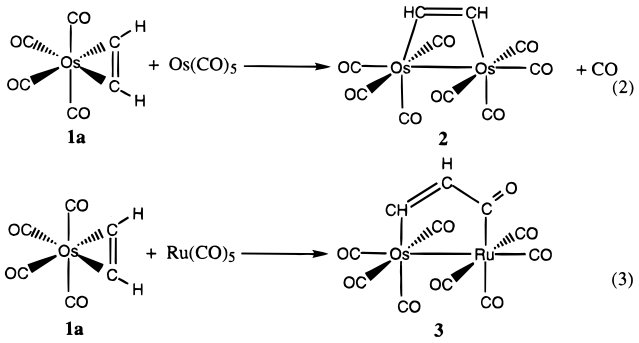

is a diosmacyclobutene, but with $Ru(CO)_5$, the product has undergone CO insertion. The synthesis and characterization of these products are reported here, along with extensive kinetic studies of these reactions. If the rate-controlling step is CO dissociation activated by the acetylene, then the kinetics of reaction 1 and of reactions 2 and 3 should be related.

Results

Synthesis of $M(CO)_4(\eta^2\text{-}C_2H_2)$ (M = Os, 1a; Ru, 1b). The tetracarbonyl−acetylene compounds **1a** and **1b** are thermally unstable solids so that low-temperature photolysis and workup are essential for their successful synthesis and isolation. A further challenge in the synthesis is that the two main CO stretching bands of the products are virtually coincident with the two ν_{CO} bands of the parent pentacarbonyls so that IR monitoring of the progress of the reaction can be judged only by the change in relative intensities of the 2036/1994 bands. The synthesis of **1a** was carried out many times and by several different co-workers. The conditions recommended in the Experimental Section should be closely followed to ensure isolation of these delicate compounds in the stated purity and yield.

As described previously[7b] and quantified in a kinetic study,[9] the carbonyl ligands in **1a** undergo rapid exchange with two-electron ligands, including ^{13}CO. This permits ^{13}CO enrichment of **1a** by simply stirring a hydrocarbon solution under ^{13}CO, a very useful feature for ^{13}C NMR characterization of the compound. Unfortunately, the acetylene ligand also is very labile in **1b**, and similar ^{13}CO enrichment is not possible. The alkyne ligand lability of **1b** resembles that of $Ru(CO)_4(\eta^2\text{-}Me_3SC_2SiMe_3)$[11] and not that of the more robust and ^{13}CO-enrichable $Ru(CO)_4(\eta^2\text{-}CF_3C_2CF_3)$.[7a,8]

The spectroscopic signatures of **1a**/**1b** are consistent with the expected trigonal bipyramidal geometry, with the η^2-acetylene ligand occupying an in-plane equatorial position. Detailed comparison of the IR and NMR data with other $M(CO)_4(\eta^2$-alkyne) compounds will be the subject of a forthcoming publication.

The important and interesting feature in the present context is that **1a** and, to a more limited extent, **1b** undergo facile reaction with the 18-electron $M(CO)_5$ compounds to yield dimetallacyclic products.

Reactions of $M(CO)_4(\eta^2\text{-}C_2H_2)$ (M = Os, 1a; Ru, 1b) with $M(CO)_5$. The reaction between $M(CO)_4(\eta^2\text{-}C_2H_2)$ and the parent pentacarbonyls proceeds readily near 0 °C and gives, after simple workup, the corresponding dimetallacycles in excellent yield (an exception is the delicate RuRu compound **4**). However, the pentacarbonyls give different types of dimetallacyclic products. As shown in eqs 2 and 3, the reaction between $Os(CO)_4(C_2H_2)$ and $Os(CO)_5$ yields diosmacyclobutene **2**, accompanied by a loss of a CO, whereas the reaction between $Os(CO)_4(C_2H_2)$ and $Ru(CO)_5$ appears to be a simple addition of two 18-electron molecules, giving dimetallacyclopentenone **3** (RuOs) or the analogous **4** (RuRu) with $Ru(CO)_4(C_2H_2)$. There is no CO loss, and the process involves both metal−metal and C−C bond formation. The spectroscopic signatures of the compounds uniquely define their structures.[12]

Compound **2** shows CO stretching bands and ^{13}CO resonances only in the terminal carbonyl region. The 2:1:1 intensity ratio of the latter signals is in accord with the C_{2v} symmetry of the molecule. The ^1H and ^{13}C chemical shifts of the μ-C_2H_2 moiety are δ 6.96 and 98.4 ppm, respectively, with a $^1J_{CH}$ of 156 Hz from the ^1H coupled ^{13}C NMR spectrum. Analysis of the AA′XX′ spin system of the $Os_2(CO)_8(\mu\text{-}^{13}C_2H_2)$ isotopomer gave values in close agreement, δ 98.25 ppm and $^1J_{CH}$ of 157.8 Hz, and allowed the determination of the $^1J_{CC}$ coupling constant, 57.2 Hz. The ^1H chemical shift (δ 6.96) is in the olefinic region and compares well with δ 7.11 and 7.80 in $Ru_2(CO)_4\{\mu\text{-}(RO)_2PN(Et)P(OR)_2\}_2(\mu\text{-}C_2H_2)$[13] and $Ru_2(CO)_4(\mu\text{-}\eta^1,\eta^1\text{-dppm})_2(\mu\text{-}C_2H_2)$,[14] respectively. The ^{13}C chemical shifts of the bridging acetylene in these compounds are at 121.1 and 136.0 ppm, respectively. The closeness of these signals to that of free ethylene (123.3 ppm) was taken as supportive of a dimetallacyclobutene formulation. The same resonance in **2** is observed at δ 98.4 ppm, between free ethylene and acetylene (71.9 ppm), and might be taken to indicate a somewhat different bonding mode. However, it is well documented[15] that the chemical shifts of carbon atoms directly bonded to transition metals are influenced by the metal, usually shifting upfield upon descending a metal triad, and further examples in **3** and **4** are described below.

In accord with the dimetallacyclopentenone formulation, the IR spectra of **3** and **4** contain, in addition to terminal carbonyl stretching bands, a medium-intensity signal at 1635 cm^{-1} in each, which is assigned to the ketonic carbonyl group. In the compound closely related to **4**, $Ru_2(CO)_4(\mu\text{-dppm})_2(\mu\text{-}\eta^1,\eta^1\text{-HCCHCO})$[14] (**5**), the corresponding band is at 1534 cm^{-1}; its low value was attributed to strong back-bonding from the electron-rich Ru center due to the presence of the two dppm phosphorus donors. Differential back-bonding to the ketonic C═O is also reflected in the ^{13}C chemical shifts. The ^{13}C NMR spectra of the ^{13}CO-enriched materials **3*** and **4*** show the ketonic carbonyl at 236.3 and 235.6 ppm,

(11) (a) Ball, R. G.; Burke, M. R.; Takats, J. *Organometallics* **1987**, *6*, 1918. (b) Ball, R. G.; Burke, M. R.; Takats, J. *Organometallics* **1988**, *7*, 1234.

(12) The structural formulations of **2** and **3** were corroborated by X-ray crystallography, but the poor quality of the crystals allowed only the determination of the atom connectivities; discussion of the metrical parameters and the implications for bonding are not warranted: Day, V. W. Unpublished results.

(13) Field, J. S.; Haines, R. J.; Sundermeyer, J.; Woollam, S. F. *J. Chem. Soc., Dalton Trans.* **1993**, 3749.

(14) Mirza, H. A.; Vittal, J. J.; Puddephatt, R. J. *Organometallics* **1994**, *13*, 3063.

(15) Mann, B. E.; Taylor, B. E. *^{13}C NMR Data for Organometallic Compounds*; Academic Press: New York, 1981.

respectively, while there is a downfield shift of almost 30 ppm to 264.9 ppm in **5**. The ^{13}C NMR spectrum of **3*** shows six terminal carbonyl signals in the expected 2:1:1:2:1:1 ratio. For labeling of these and other signals see the diagram.

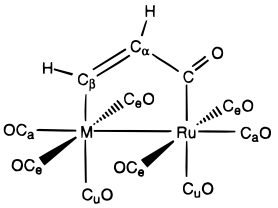

M = Os(**3**), Ru(**4**)

The lower field signals are assigned to Ru carbonyls:[15] 198.9 ($2CO_e$), 190.9 ($1CO_u$), 183.4 ($1CO_a$). The doublet appearance of the signal at 190.9 and that of the ketonic carbonyl ($^2J_{RuCOu-C=O}$ = 18 Hz) establishes their trans relationship and secures the assignment of $RuCO_u$. Assignment of the remaining Ru-carbonyls follows from the relative intensities of the signals. The high-field carbonyl peaks belong to osmium: 182.9 ($2CO_e$), 173.2 ($1CO_u$), 165.5 ($1CO_a$). The signal at 173.2, assigned to CO_u, is a singlet in **3*** but becomes a doublet in **3**** (prepared with ^{13}CO and $^{13}C_2H_2$), due to coupling to the Os-bonded trans-$^{13}C_\beta H$, ($^2J_{OsCOu-CH}$ = 15 Hz). As above, this completes the carbonyl assignments on osmium. The observation that the ketonic carbonyl is attached exclusively to ruthenium indicates that the reaction is highly regioselective. As expected from the dimetallacyclopentenone formulation, two CH resonances are observed in both the ^1H and ^{13}C NMR spectra. The H_α/C_α and H_β/C_β signals are at 8.17/166.5 and 7.46/131.4 ppm, respectively. The assignments were secured from selective $^{13}C\{^1H\}$ experiments and from the one-bond $^{13}C-^{13}C$ coupling of 39 Hz in **3**** between the ketonic carbonyl resonance and C_α (165.4 ppm in CD_3CN). The latter spectrum also revealed the one-bond $J_{C\alpha-C\beta}$ coupling as 62 Hz and $^1J_{CH}$ of 155 and 150 Hz, respectively. The influence of the metal on the ^{13}C chemical shift of directly bonded carbon atoms is illustrated by comparing the data between **3** and **5**. The position of the C_α resonance in **3** (166.5 ppm) compares well with that in **5** (170.8 ppm); however the C_β signal (131.4 ppm) again has moved upfield by more than 30 ppm from its position in **5** (176.8 ppm), reflecting the change from Ru*C*H in **5** to Os*C*H in **3**. We have already noted similar ~30 ppm upfield shifts for the ketonic carbon in **3** compared to **5** and the μ-C_2H_2 carbons in **2** compared to its Ru analogues.[13,14] Unfortunately, due to the delicate nature of **4**, confident identifications of the C_α, C_β resonances in this compound could not be made and a direct comparison between the $Ru-C_\beta$ signals in **4** and **5** is not available.

It has been argued[16] that one-bond C−H and especially C−C coupling constants are better indicators of the nature of bridging hydrocarbyl ligand than ^{13}C chemical shifts. The magnitudes of $^1J_{CC}$ and $^1J_{CH}$ in **2** are greatly reduced from those of free acetylene[17] (171.5 and 249 Hz, respectively) and are close to those of free ethylene[17] (67.6 and 156 Hz, respectively) and support the diosmacyclobutene formulation for **2**. In fact, the $^1J_{CC}$ in **2** (57.2 Hz) is smaller than that of free ethylene. This might be due to ring strain, as suggested by Norton,[16] since the length of the Os−Os bond clearly introduces strain into the four-membered heterocyclic core. Similarly, the values of $^1J_{CC}$ and $^1J_{CH}$ in **3** (61 and 155, 149 Hz, respectively) and **5** (57 and 144, 134 Hz, respectively) are similar to those of free ethylene and provide good evidence for the localized C=C bond in **3**. The $^1J_{C\alpha-C\equiv O}$ of 39 Hz in **3** is closer to that in ethane (34.6 Hz) and infers a quite different state for the ketonic carbon.

A final point of interest concerning the behavior of compounds **2**, **3**, and **4** is the question of exchange of carbonyl ligands between the two ends of the molecule. Intramolecular carbonyl scrambling between metals in di- and polynuclear metal carbonyls is a well-known phenomenon.[18] A common mechanism for carbonyl migration is the so-called "merry-go-round" process, which exchanges terminal carbonyls between two or more centers via a symmetrical doubly bridged intermediate.[18b] This is illustrated clearly by the hexafluorobutyne-bridged analogues of **2**, $MM'(CO)_8(\mu\text{-}\eta^1,\eta^1\text{-}CF_3CCCF_3)$ (M = M′ Ru, Os; M = Ru, M′ = Os),[7a] which also exhibited the normal metal dependence of fluxionality; the facility for carbonyl scrambling is RuRu > RuOs > OsOs. This behavior is mirrored by the present compounds. The ^{13}C carbonyl signals of compound **2** are sharp at room temperature and attest to its rigid, nonfluxional nature. The ^{13}C NMR spectra of compounds **3** and **4** are temperature dependent. The sharp carbonyl signals observed at −86 °C for **3** experience selective broadening at room temperature. The signals at 236.3 (RuC=O), 190.9 ($RuCO_u$), and 173.2 ($OsCO_u$) ppm remain sharp, whereas the other resonances are broad. This is consistent with the onset of the merry-go-round process that exchanges the six coplanar carbonyl ligands, $2CO_e$ and $1CO_a$, on Ru and Os. The observation that one terminal carbonyl signal on Ru and Os remains sharp provides further confirmation of their assignment as the unique carbonyl ligands opposite the dimetallacyclopentenone ring. As expected, compound **4** is the most fluxional of the three. As the temperature is raised from −80 °C, four of the carbonyl signals broaden, while those at 235.6 (RuC=O) and 191.6 (overlapping $RuCO_u$ and $RuCO_{u'}$) remain sharp. At 30 °C carbonyl exchange is sufficiently fast as to produce a sharp averaged signal for the four exchanging sites at 196.1 ppm, the RuC=O resonance is at 232.6 ppm, and the $RuCO_u$ and $RuCO_{u'}$ signals now are resolved at 192.2 and 192.0 ppm.

^{13}C NMR Monitoring of the Reaction between $Os(CO)_4(C_2H_2)$ and $Ru(CO)_5$. To investigate the mechanism of formation of the dimetallacyclopentenone products, which formally involves simple addition of two 18-electron partners, the reaction of $Os(CO)_4(C_2H_2)$ and $Ru(CO)_5$ was carried out with different permutations

(16) Bender, B. R.; Norton, J. R.; Miller, M. M.; Anderson, O. P.; Rappé, A. K. *Organometallics* **1992**, *11*, 3427.

(17) Levy, G. C.; Nelson, G. N. *Carbon-13 Nuclear Magnetic Resonance for Organic Chemistry*; Wiley: New York, 1972; Chapter 2, pp 28−29, Tables 2.3 and 2.4.

(18) (a) Mann, B. E. *J. Chem. Soc., Dalton Trans.* **1997**, 1457. (b) Bond, E.; Muetterties, E. L. *Chem. Rev.* **1978**, *78*, 635. (c) Adams, R. D.; Cotton, F. A. In *Dynamic Nuclear Magnetic Resonance Spectroscopy*; Jackman, L. M., Cotton, F. A., Eds.; Academic Press: New York, 1975; Chapter 12.

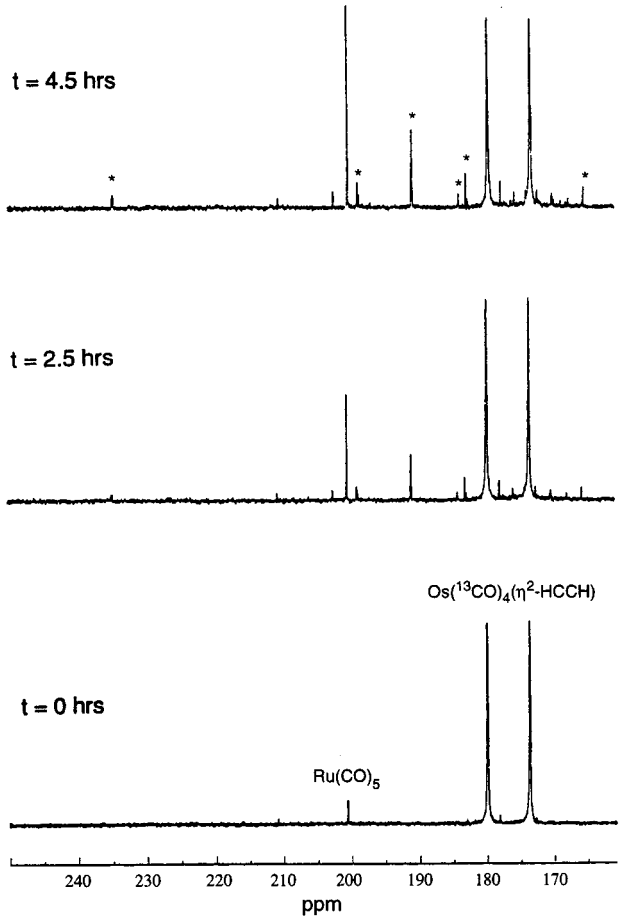

Figure 1. Time dependence of the $^{13}C\{^1H\}$ NMR spectrum of the reaction of $Os(^{13}CO)_4(\eta^2\text{-}C_2H_2)$ with $Ru(CO)_5$ in dichloromethane at −25 °C. Product peaks are indicated by a *.

of ^{13}CO-enriched reactants and ultimately monitored by low-temperature ^{13}C NMR spectroscopy.

With the naive expectation that specifically labeled **3** might be obtained from specifically labeled starting materials, the reactions of $Ru(^{13}CO)_5$ with $Os(CO)_4(C_2H_2)$ and $Ru(CO)_5$ with $Os(^{13}CO)_4(C_2H_2)$ were carried out under "benchtop" conditions. However, ^{13}C NMR spectra of the isolated products showed complete carbonyl scrambling between Ru and Os.

Monitoring the reaction by low-temperature ^{13}C NMR spectroscopy in dichloromethane revealed some interesting details of the reaction. The time profile of the reaction between $Os(^{13}CO)_4(C_2H_2)$ and $Ru(CO)_5$ at −25 °C is shown in Figure 1. After 2.5 h and more clearly after 4.5 h, formation of small amounts of product is observed, but notably, at the same time and at a somewhat faster rate, ^{13}CO enrichment of $Ru(CO)_5$ also occurs. The incorporation of ^{13}CO into $Ru(CO)_5$ is an interesting observation. The thermal exchange of CO with $Ru(CO)_5$ is known to be a slow process,[19] and this we verified by monitoring the ^{13}C NMR spectrum of $Ru(CO)_5$ under an atmosphere of ^{13}CO at −25 °C. No ^{13}CO enrichment of $Ru(CO)_5$ was observed after 4.5 h, within the normal detection limits and errors of NMR measurements. Therefore it is clear that the ^{13}CO incorporation into $Ru(CO)_5$ seen in the present case

(19) Huq, R.; Poë, A. J.; Chawla, S. *Inorg. Chim. Acta* **1980**, *8*, 374.

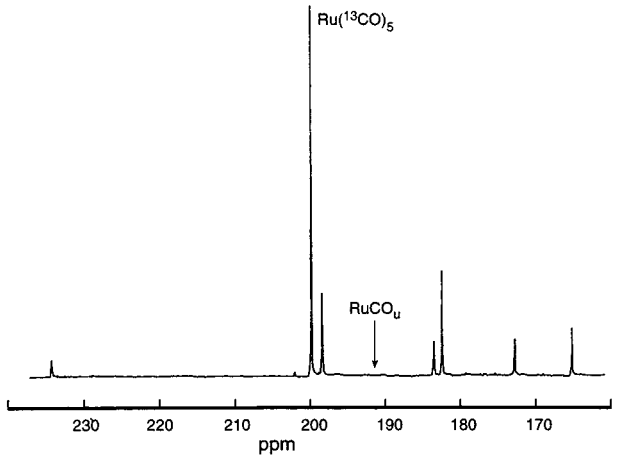

Figure 2. $^{13}C\{^1H\}$ NMR spectrum of the product of the reaction of $Os(CO)_4(\eta^2\text{-}C_2H_2)$ with $Ru(^{13}CO)_5$ after 2 h in dichloromethane at −25 °C.

must be facilitated in some fashion by the osmium−alkyne compound **1a**. Another feature of the reaction is that, although formation of **3** is accompanied by incorporation of ^{13}CO in all terminal carbonyl and ketonic carbonyl sites, the strongest product peak is at 192.2 ppm; the one assigned to the CO ligand on Ru trans to the ketonic CO group. On the other hand, the ^{13}C NMR spectrum of the reaction between $Os(CO)_4(C_2H_2)$ and $Ru(^{13}CO)_5$ at −25 °C after 2 h, Figure 2, did not show incorporation of ^{13}CO into $Os(CO)_4(C_2H_2)$ and revealed all of the signals expected for product **2**, except for that at 192.2 ppm. The mechanistic implications of these observations are discussed below in conjunction with the overall mechanism. It should be noted that product formation is far from complete in these experiments, being about 10% after 1.5 h and 20% after 4.5 h, estimated from the kinetic measurements described below.

Reaction Kinetics. The results described above show that $Os(CO)_4(\eta^2\text{-}C_2H_2)$ undergoes facile condensation reactions with $Os(CO)_5$ and $Ru(CO)_5$, but the two pentacarbonyls give different products **2** and **3**, as shown in reactions 2 and 3.

Kinetic monitoring of these reactions is somewhat confined because much of the carbonyl region of the infrared spectrum is obscured by the $M(CO)_5$ reactant that is present in excess. However, it is possible to follow the formation of the product at 2083 cm^{-1} (M = Os) or 2089 cm^{-1} (M = Ru) without significant interference from $M(CO)_5$. Nevertheless, it was necessary to study the reactions with less than a pseudo-first-order excess of $M(CO)_5$. The reaction conditions for $Ru(CO)_5$ and $Os(CO)_5$ are summarized in Tables 1 and 2, respectively.

These reactions have some obvious formal analogies, but they show distinct qualitative kinetic differences. With $Ru(CO)_5$, all of the absorbance−time curves can be fitted by a first-order rate law for concentration ratios of $Ru(CO)_5$:$Os(CO)_4(\eta^2\text{-}C_2H_2)$ from 2:1 to 10:1. Representative data are shown in Figures 3 and 4, and the results are summarized in Table 1. The first-order rate constants (k_1) are close to those for the reaction of $Os(CO)_4(\eta^2\text{-}C_2H_2)$ with PMe_3, being essentially the same below −5 °C and 15−20% smaller at 0−10 °C. This provides a strong hint that the rate-controlling step is CO dissociation from $Os(CO)_4(\eta^2\text{-}C_2H_2)$. The rate is

Table 1. Kinetic Results for the Reaction of $Os(CO)_4(\eta^2\text{-}C_2H_2)$ with $Ru(CO)_5$ in Pentane

T, °C	[**1**] $\times 10^3$, M	[$Ru(CO)_5$] $\times 10^3$, M	[CO][a] $\times 10^3$, M	$10^4 \times k_1$[b], s^{-1}	$10^3 \times k_4$[c], s^{-1}	$\frac{(k_{-2}+k_3)k_{-1}}{k_2 k_3}$[c]
10.0	0.421	2.16	0	35.6 (41.0)	9.5	(0.90)
10.0	0.421	2.16	0	33.9 (41.0)	9.0	(0.90)
5.2	0.421	2.16	0	18.4 (20.8)	7.2	(0.90)
5.2	0.421	4.32	0	19.9 (20.8)	7.8	(0.90)
5.2	1.24	3.74	7.0	6.91 (20.8)	(7.8)	0.90
5.0	0.421	0.864	0	16.3 (20.2)	7.2	(0.90)
5.0	0.421	2.16	0	15.5 (20.2)	6.8	(0.90)
5.0	1.26	2.16	0	17.4 (20.2)	7.2	(0.90)
5.0	0.421	4.32	0	17.1 (20.2)	7.0	(0.90)
5.0	0.421	4.32	0	17.0 (20.2)	7.5	(0.90)
0.0	1.26	3.46	7.0	3.73 (9.66)	(6.0)	0.80
0.0	1.26	3.46	7.0	3.76 (9.66)	(6.0)	0.75
0.0	0.421	4.32	7.0	4.35 (9.66)	(6.0)	0.75
0.0	0.421	4.32	7.0	4.37 (9.66)	(6.0)	0.80
−5.0	0.421	0.864	0	4.17 (4.51)	4.8	(0.75)
−5.0	1.26	2.16	0	4.13 (4.51)	4.2	(0.75)
−5.0	0.421	4.32	0	4.14 (4.51)	4.5	(0.75)
−5.0	1.24	3.74	7.0	1.82 (4.51)	(4.5)	0.85
−5.0	1.24	3.74	7.0	1.56 (4.51)	(4.5)	0.75
−5.1	0.421	2.16	0	4.71 (4.40)	5.2	(0.75)
−9.3	1.26	2.16	0	2.12 (2.29)	3.0	(0.75)

[a] A 0 entry indicates no added CO; otherwise the run is in pentane saturated with CO at 1 atm. [b] Apparent first-order rate constant determined from the absorbance change at 2089 cm^{-1}; values in parentheses are calculated from the PMe_3 substitution in pentane. [c] Entries in parentheses indicate that the parameter is not defined under the reaction conditions and the value has been assumed based on other runs.

Table 2. Kinetic Results for the Reaction of $Os(CO)_4(\eta^2\text{-}C_2H_2)$ with $Os(CO)_5$ in Pentane

T, °C	[**1**] $\times 10^3$ M	[$Os(CO)_5$] $\times 10^3$ M	[CO][a] $\times 10^3$ M	$10^3 \times \epsilon_P$[b], M cm^{-1}	$\frac{(k_{-2}+k_3)k_{-1}}{k_2 k_3}$[c]
15.2	0.643	2.10	0	10.7	65
15.2	0.810	2.10	0	10.7	75
15.0	0.643	1.38	0	10.5	77
15.0	0.643	2.75	0	10.8	80
15.0	0.643	6.88	0	9.80	75
15.0	0.643	10.3	0	10.3	67
15.0	0.643	11.0	0	10.4	67
15.0	0.643	13.8	0	10.3	68
15.0	1.24	3.44	7.0	10.1	67
15.0	1.24	3.44	7.0	10.2	67
10.0	0.643	6.88	0	10.5	65
10.0	1.24	3.44	7.0	10.1	70
10.0	1.24	3.44	7.0	10.3	68
5.2	0.643	6.88	0	10.6	64
0.5	0.480	6.88	0	10.2	58
0.0	1.08	3.44	0	10.5	60
0.0	0.875	3.44	7.0	10.4	58
0.0	0.875	3.44	0	10.5	55
0.0	0.875	3.44	7.0	10.5	58
0.0	0.845	3.44	0	10.3	62
0.0	0.845	3.44	7.0	10.0	65
−0.1	0.643	6.88	0	10.8	65
−5.0	0.643	6.88	0	11.3	60

[a] A 0 entry indicates no added CO; otherwise the run is in pentane saturated with CO at 1 atm. [b] Molar extinction coefficient of the product, **2**, determined from the best visual fits to the model described in the text. [c] The rate constant coefficient defined by the model and used as the only adjustable kinetic parameter in determining the best visual fits; based on the sensitivity of the fit, the uncertainty is estimated to be ±5%, while ignoring uncertainties in concentrations and temperature.

almost independent of the $Ru(CO)_5$ concentration, but is always slower in pentane saturated with CO. All of these features are illustrated in Figures 3 and 4.

The kinetics of the reaction with $Os(CO)_5$ show several significant differences. The absorbance−time curves are not adequately fitted by a first-order rate law. Some examples are shown in Figure 5, where it can be seen that the initial rapid product formation seems to be followed by a slower stage. Another difference, also

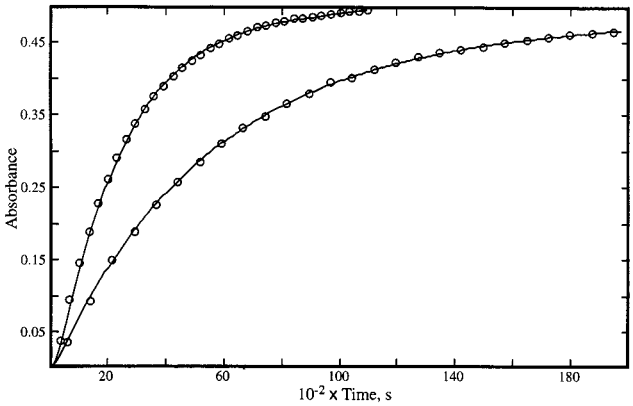

Figure 3. Absorbance−time curves for the reaction of $Os(CO)_4(\eta^2\text{-}C_2H_2)$ with $Ru(CO)_5$ in pentane at −5.0 °C. The initial concentrations (M) of $Os(CO)_4(\eta^2\text{-}C_2H_2)$, $Ru(CO)_5$, and CO, respectively, are 1.26×10^{-3}, 2.16×10^{-3}, and 0 (upper curve); 1.24×10^{-3}, 3.74×10^{-3}, and 7.0×10^{-3}. The curves are fits to the model described in the text.

illustrated in Figure 5, is that the rate increases very significantly with increasing concentrations of $Os(CO)_5$.

The effect of added CO is much more dramatic with $Os(CO)_5$ compared to $Ru(CO)_5$. In CO-saturated pentane, the rate decreases by 2−2.5-fold with $Ru(CO)_5$ (Figures 3 and 4), but by 7−10-fold with $Os(CO)_5$ (Figure 6). This provides an indication that the non-first-order behavior with $Os(CO)_5$ may be because CO is produced during the reaction and its inhibitory effect will increase as the concentration of CO increases during the reaction.

A consideration of these qualitative observations and the quantitative analysis described below suggest the reaction pathway shown in Scheme 1 as the simplest one that is consistent with the kinetic observations.

Scheme 1 proposes that the reaction is initiated by CO dissociation from $Os(CO)_4(\eta^2\text{-}C_2H_2)$, as would be consistent with the similarity in rates to those for PMe_3 substitution, especially for the $Ru(CO)_5$ reaction. The

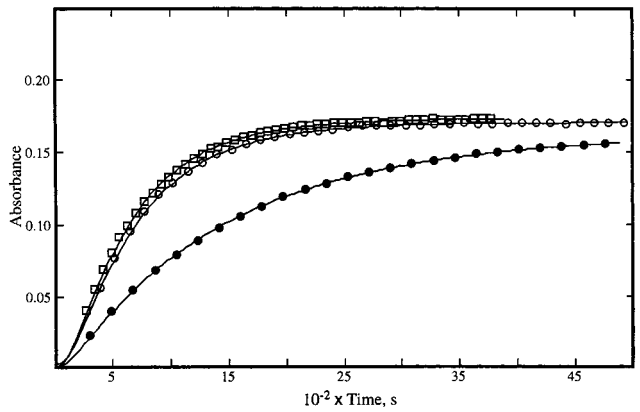

Figure 4. Absorbance−time curves for the reaction of $Os(\eta^2\text{-}CO)_4(C_2H_2)$ with $Ru(CO)_5$ in pentane. The initial concentrations (M) of $Os(CO)_4(\eta^2\text{-}C_2H_2)$, $Ru(CO)_5$, and CO, respectively, are 0.421×10^{-3}, 0.864×10^{-3}, and 0 at 5 °C (○); 0.421×10^{-3}, 4.32×10^{-3}, and 0 at 5 °C (□); 1.24×10^{-3}, 3.74×10^{-3}, and 7.0×10^{-3} at 5.2 °C, with actual absorbances divided by 3 (●). The curves are fits to the model described in the text.

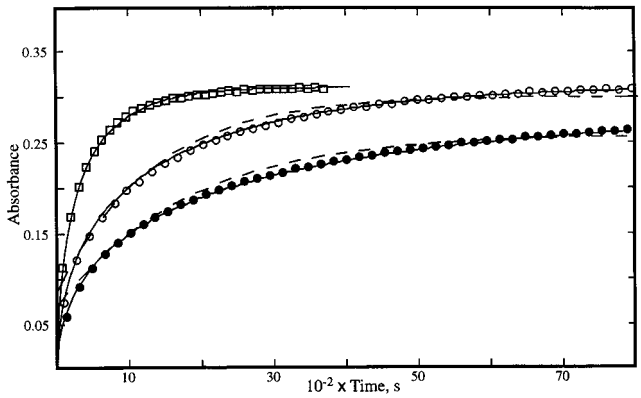

Figure 5. Absorbance−time curves for the reaction of $Os(CO)_4(\eta^2\text{-}C_2H_2)$ (6.43×10^{-4} M) with varying $Os(CO)_5$ concentrations of 1.38×10^{-3} M (●), 2.75×10^{-3} M (○), and 10.3×10^{-3} M (□), monitored at 2083 cm^{-1} and 15 °C. Dashed curves are least-squares best fits to a first-order rate law; solid curves are visual fits to the model described in the text. For clarity, every second experimental point is shown for (●) and (○) and every third for (□).

unsaturated intermediate $\{Os(CO)_3(\eta^2\text{-}C_2H_2)\}$ may react with CO to give reactant (k_{-1}) or with $M(CO)_5$ (k_2), and the CO inhibition would result from the competition between these two processes. The most plausible product of the k_2 step is the dative metal−metal bonded species **6**, where the $M(CO)_5$ acts as a two-electron Lewis base. Although unbridged donor−acceptor bonds between metals are rare, their number is growing.[20] The

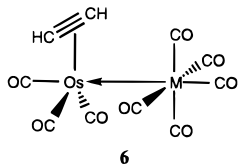

6

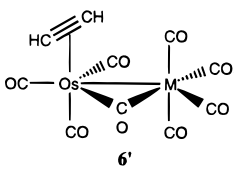

6'

intermediacy of these species is suggested by the previously described intermolecular CO exchange between $Ru(CO)_5$ and $Os(^{13}CO)_4(\eta^2\text{-}C_2H_2)$ that occurs at a rate competitive with final product formation. This can occur as a result of CO scrambling between metals via **6′**, a known process, and the reversibilty of the k_2 step. As a supportive observation, we note that Vrieze et al.[21] in their detailed study of the $Ru(CO)_4(PMe_2Ph)$-catalyzed carbonylation of $Ru(CH_3)X(CO)_2(DAB)$ (DAB = substituted diazadienes, X = halide) also observed intermolecular CO scrambling between the reactants, albeit at a higher temperature (45 °C) than in the present case, and demonstrated the intermediacy of a dimetallic species, either $[Ru(CH_3)X(CO)(DAB)Ru(CO)_3(PMe_2Ph)(\mu\text{-}CO)_2]$ or $[Ru(CH_3)(CO)_2(DAB)Ru(CO)_4(PMe_2Ph)]^+$. The latter, with an unbridged donor−aceptor metal−metal bond, is clearly analogous to **6**. The intermediate **6** then reacts by the k_3 step to give the final product. This last step would be as shown in Scheme 1 for $Os(CO)_5$, but must involve insertion and consumption of one CO for $Ru(CO)_5$.

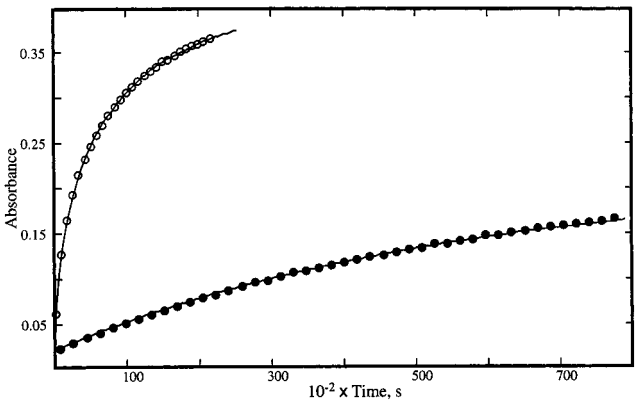

Figure 6. Absorbance−time curves for the reaction of $Os(CO)_4(C_2H_2)$ with $Os(CO)_5$ in pentane at 0.0 °C, with initial CO concentrations of 0 (○) and 7.0×10^{-3} M (●). The initial concentrations of $Os(CO)_4(\eta^2\text{-}C_2H_2)$ and $Os(CO)_5$ are 0.875 $\times 10^{-3}$ and 3.44×10^{-3} M, respectively. The curves are fits to the model described in the text.

Scheme 1

$$Os(CO)_4(\eta^2\text{-}C_2H_2) \underset{k_{-1}}{\overset{k_1}{\rightleftharpoons}} \{Os(CO)_3(\eta^2\text{-}C_2H_2)\} + CO$$

$$\{Os(CO)_3(\eta^2\text{-}C_2H_2)\} + M(CO)_5 \underset{k_{-2}}{\overset{k_2}{\rightleftharpoons}} \{Os(CO)_3(\eta^2\text{-}C_2H_2)M(CO)_5\}$$

$$\{Os(CO)_3(\eta^2\text{-}C_2H_2)M(CO)_5\} \xrightarrow{k_3} \text{Product}$$

From Scheme 1, a steady-state assumption for the intermediates $\{Os(CO)_3(\eta^2\text{-}C_2H_2)\}$ and $\{Os(CO)_3(\eta^2\text{-}C_2H_2)M(CO)_5\}$ yields the rate law given by eqs 4 and 5.

$$\text{Rate} = \frac{k_1k_2k_3[Os(CO)_4(C_2H_2)][M(CO)_5]}{(k_{-2} + k_3)k_{-1}[CO] + k_2k_3[M(CO)_5]} \quad (4)$$

$$= \frac{k_1[Os(CO)_4(C_2H_2)]}{\dfrac{(k_{-2} + k_3)k_{-1}[CO]}{k_2k_3[M(CO)_5]} + 1} \quad (5)$$

(20) Jiang, F.; Male, J. L.; Biradha, K.; Leong, W. K.; Pomeroy, R. K.; Zaworotko, M. J. *Organometallics* **1998**, *17*, 5810, and references therein.

(21) (a) Kraakman, M. J. A.; de Klerk-Engels, B.; de Lange, P. P. M.; Vrieze, K. *Organometallics* **1992**, *11*, 3774. (b) de Klerk-Engels, B.; Groen, J. H.; Kraakman, M. J. A.; Ernsting, J. M.; Vrieze, K. *Organometallics* **1999**, *13*, 3279.

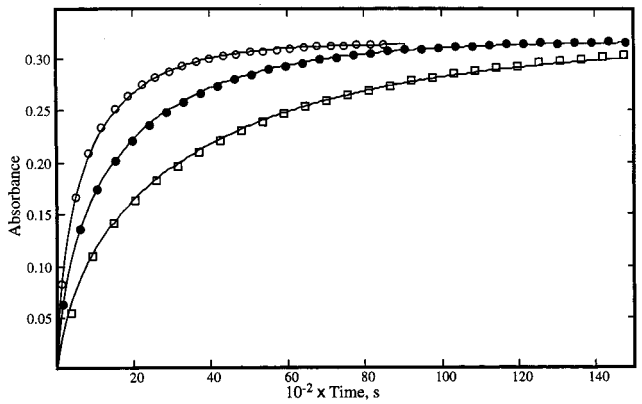

Figure 7. Absorbance−time curves for the reaction of $Os(CO)_4(\eta^2\text{-}C_2H_2)$ with $Os(CO)_5$ in pentane at temperatures of 10.0 (○), 5.2 (●), and −0.1 °C (□). The initial concentrations of $Os(CO)_4(\eta^2\text{-}C_2H_2)$ and $Os(CO)_5$ are 0.643×10^{-3} and 6.88×10^{-3} M, respectively. The curves are fits to the model described in the text.

If this rate law is to apply to both the $Ru(CO)_5$ and $Os(CO)_5$ systems, there must be some quantitative difference to explain their different kinetic behavior. For $Ru(CO)_5$, the rate law is consistent with the observations if the first term in the denominator of eq 5 is <1 for most of the kinetic conditions. But with $Os(CO)_5$ this term must be ≥1 so that the rate shows some dependence on $Os(CO)_5$ and more inhibition by CO. The fact that $Os(CO)_5$ shows much more inhibition in pentane saturated with CO implies that the rate constant quotient in the denominator of eq 5 is larger for $Os(CO)_5$. The complications and consequences of the consumption of CO during the k_3 step with $Ru(CO)_5$ are discussed below.

The above qualitative analysis provides the justification for proceeding to fit the data to the model in Scheme 1. This fitting process has been done by numerical integration of the differential equations based on Scheme 1. This was necessary because many runs are not under pseudo-first-order conditions since a large excess of $M(CO)_5$ masks the infrared region where the product is observed. Furthermore, the CO is produced at steady-state amounts with $Ru(CO)_5$ and at concentrations similar to that of the $Os(CO)_4(\eta^2\text{-}C_2H_2)$ with $Os(CO)_5$. The latter is true even in CO-saturated pentane because of the limited solubility of CO.

The numerical integration procedure was done with the major constraint that k_1 has the value predicted from the phosphine substitution reaction. Then, as can be seen from eq 5, the only kinetic fitting parameter is the ratio $(k_{-2} + k_3)k_{-1}/k_2k_3$. This ratio should be constant for all runs at a particular temperature and probably is not very temperature dependent. Therefore the temperature dependence of the fits is further constrained to correspond to the previously determined temperature dependence of k_1.

The results of this analysis for $Os(CO)_5$ are summarized in Table 2, where the values of $(k_{-2} + k_3)k_{-1}/k_2k_3$ and the molar extinction coefficient of the product are values that gave the best visual fit. Representative fits for the reaction of $Os(CO)_4(\eta^2\text{-}C_2H_2)$ with $Os(CO)_5$ are shown in Figures 5−7. Because CO is produced by this reaction, the amount of CO present during the reaction is defined by the stoichiometry and is not dependent on k_3. The effect of saturating the pentane with CO is shown by the results in Figure 6. It is clear that the model and these parameters give an excellent fit for the concentration and temperature dependence of the absorbance−time curves and give an average for $(k_{-2} + k_3)k_{-1}/k_2\ k_3 \approx 70$.

Scheme 2

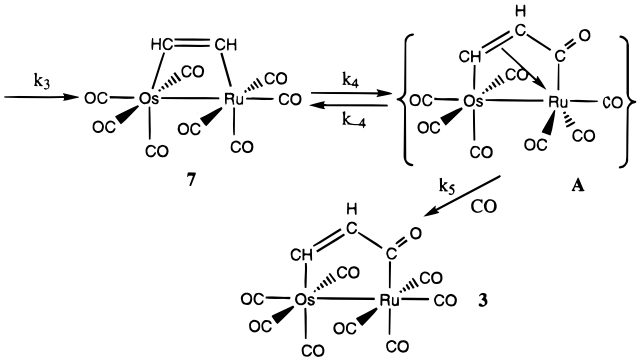

It should be noted that, for the very slow reactions with CO added and especially below 0 °C, the final absorbance of product appeared to be lower than expected from other runs. This effect is attributed to some spontaneous decomposition of $Os(CO)_4(\eta^2\text{-}C_2H_2)$, as confirmed by blank experiments with only $Os(CO)_4(\eta^2\text{-}C_2H_2)$ as the reactant. The final model included this effect with spontaneous decomposition rate constants of 3.7×10^{-5}, 2.4×10^{-5}, 1.5×10^{-5}, and 9.0×10^{-6} s^{-1} at 15, 10, 5, and 0 °C, respectively, for all the runs.

The results of the analysis for $Ru(CO)_5$ are summarized in Table 1. The analysis of this system requires some modification of Scheme 1 because CO is produced and then consumed in the net reaction. This could be accounted for by the k_3 step being dependent on [CO] and replacing k_3 with k_3[CO] in eqs 4 and 5. However, the steady-state assumption for the intermediates in Scheme 1 requires that the CO concentration is so low that it could not account for the small inhibition and still be consistent with the 2−2.5-fold inhibition observed in pentane saturated with CO. Therefore the k_3 step must be independent of [CO] and the return of the CO must be at a later stage. This is consistent with the extension of Scheme 1 shown in Scheme 2, in which the product of the k_3 step undergoes insertion to give the final product and the CO is involved at the final stage.

If a steady state is assumed for the intermediate **A**, then the rate of production of CO and product are given by eqs 6 and 7, respectively.

$$\frac{d[CO]}{dt} = \frac{d[\mathbf{7}]}{dt} = \frac{k_1[Os(CO)_4(C_2H_2)]}{\dfrac{(k_{-2} + k_3)k_{-1}[CO]}{k_2k_3[M(CO)_5]} + 1} - \frac{k_4[CO][\mathbf{7}]}{\dfrac{k_{-4}}{k_5} + [CO]} \tag{6}$$

$$\frac{d[\mathbf{3}]}{dt} = \frac{k_4[CO][\mathbf{7}]}{\dfrac{k_{-4}}{k_5} + [CO]} \tag{7}$$

Clearly this introduces an annoying number of potential parameters into the analysis of the absorbance−time curves with $Ru(CO)_5$. In the preliminary analysis

to establish the magnitudes of these parameters, it was assumed that the runs with and without added CO would give different limiting conditions for the rate law. In pentane saturated with CO, the steady-state amount of CO is well defined and relatively independent of the value of k_4, and it seems probable that $[CO] \gg k_{-4}/k_5$. Then the rate expressions are given by eq 8, and one can obtain an estimate of the ratio $(k_{-2} + k_3)k_{-1}/k_2\ k_3$. In addition, limits for k_4 can be obtained because its magnitude affects the induction period for the production of **7**, and we know that the delay between mixing and initial observation is 3−4 min.

$$\frac{d[CO]}{dt} = \frac{d[\mathbf{7}]}{dt} \approx \frac{k_1[Os(CO)_4(C_2H_2)]}{\frac{(k_{-2} + k_3)k_{-1}[CO]}{k_2k_3[M(CO)_5]} + 1}$$

$$\frac{d[\mathbf{3}]}{dt} \approx k_4[\mathbf{7}] \qquad (8)$$

On the other hand, if no CO is added, the concentration of CO is very small so that terms containing [CO] in the denominator of eqs 6 and 7 are probably small, and the rate expressions will be given by eq 9.

$$\frac{d[CO]}{dt} = \frac{d[\mathbf{7}]}{dt} \approx k_1[Os(CO)_4(C_2H_2)] - \frac{k_4k_5[CO][\mathbf{7}]}{k_{-4}}$$

$$\frac{d[\mathbf{3}]}{dt} \approx \frac{k_4k_5[CO][\mathbf{7}]}{k_{-4}} \qquad (9)$$

Then one can obtain limits for k_4k_5/k_{-4}, as was done for k_4 in the previous case. The ratio can be combined with k_4 to obtain an estimate of k_{-4}/k_5 that can be substituted into eqs 6 and 7 to give parameters for the full rate law. This analysis served to establish the following estimates: $(k_{-2} + k_3)k_{-1}/k_2k_3 \approx 0.8$; $0.5 \times 10^{-2} < k_4 < 2 \times 10^{-2}\ s^{-1}$; $1 \times 10^2 < k_4k_5/k_{-4} < 4 \times 10^2\ M^{-1}\ s^{-1}$ at 5.2 °C. Then one can estimate that $k_{-4}/k_5 \approx 5 \times 10^{-5}$. With these values, one can proceed to analyze the data with the full rate law (eqs 6 and 7). The final analysis used the further restrictions that k_4 would have a normal temperature dependence, but k_{-4}/k_5 was assumed to be temperature independent.

The parameters resulting from these fits are summarized in Table 1, and some representative results are shown by the curves in Figures 3 and 4. For the final analysis, a value of $k_{-4}/k_5 = 3 \times 10^{-5}$ was found to give a reasonable temperature dependence of k_4, but it must be noted that this is quite approximate, and variation by a factor of 2 would not destroy the general quality of the fits. The temperature dependence of k_4 gives activation enthalpy and entropy values of 29.7 ±2.2 kJ mol^{-1} and −178 ± 8.0 J $mol^{-1}\ K^{-1}$. As can be seen from Table 1, the model gives an average value of $(k_{-2} + k_3)k_{-1}/k_2k_3 \approx 0.8$ with a variation of ∼0.1 between different runs. This is clearly much different from the value of ∼70 obtained with $Os(CO)_5$.

Discussion

Previous studies[7−9] have shown that alkyne ligands in $M(CO)_4(\eta^2\text{-alkyne})$ (M = Fe, Ru, Os) compounds greatly activate CO dissociation relative to the $M(CO)_5$ parent, and this has been attributed to stabilization of the dissociative intermediate by four-electron donation from the alkyne as illustrated in **8**. The dissociation of

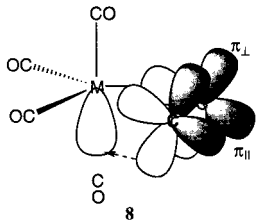

8

CO also appears to be the initial step in the reactions of $Os(CO)_5$ and $Ru(CO)_5$ with $Os(CO)_4(\eta^2\text{-}C_2H_2)$. However, the kinetics are more complex than simple phosphine substitution because of competition between CO and $M(CO)_5$ for **8**, as described by the reaction pathway in Scheme 1. This Scheme has proven to be entirely consistent with the observations in that it predicts the temperature dependence of the rate expected from the phosphine substitution studies and gives consistent results for the competition between CO and $M(CO)_5$ for the initial intermediate.

The major surprise in the kinetics of the reactions with $Os(CO)_5$ and $Ru(CO)_5$ is their quite different reactivity in steps following the formation of the intermediate in Scheme 1, as reflected in the values of $(k_{-2} + k_3)k_{-1}/k_2k_3$. If one assumes that $k_3 \gg k_{-2}$, then this ratio reduces to k_{-1}/k_2, which gives the relative rate of reaction of CO and $M(CO)_5$ with the dissociative intermediate. For nucleophiles such as phosphines,[22] this ratio typically is of the order of magnitude of 1, so that the value of 0.8 for $Ru(CO)_5$ seems rather normal, but the value of 70 for $Os(CO)_5$ implies that the latter is unusually unreactive in competition with CO. This is contrary to expectations. It is generally accepted that the basicity of transition-metal complexes increases down a triad,[23] and this is corroborated by the much greater propensity of $Os(CO)_5$ and its derivatives to form unbridged donor−acceptor metal−metal bonded species than the analogous ruthenium compounds.[20] This is particularly pertinent in the present context since formation of such a species, **6**, appears to be a prerequisite for product formation. In view of the more electron-rich nature of $Os(CO)_5$, it might have been expected that k_2 would be larger, but apparently k_2 is actually about 100 times smaller than that for $Ru(CO)_5$. However, the assumption that $k_3 > k_{-2}$ is probably not correct because, as described above, intermolecular exchange of CO between reactants is competitive with product formation. With the opposite assumption, the ratio becomes $k_{-1}k_{-2}/k_2k_3$, and if k_{-1}/k_2 is similar for both pentacarbonyls, then the observations imply either a much larger k_{-2} or a much smaller k_3 for $Os(CO)_5$.

Both intermolecular exchange of CO and formation of the final product from the presumed intermediate(s) require the formation of carbonyl-bridged species. This permits carbonyl scrambling between metals and the requisite transfer of a CO ligand from $M(CO)_5$ to the $M'(CO)_3(C_2H_2)$ unit of the dimetallic intermediate(s). The greater reluctance of third-row transition metals

(22) Chen, L.; Poë, A. J. *Inorg. Chim. Acta* **1995**, *240*, 399.
(23) Angelici, R. J. *Acc. Chem. Res.* **1995**, *28*, 51.

to support bridging carbonyls[24] will contribute, if not to a faster k_{-2} step, certainly to a slower product-forming step, k_3, for the Os−Os system. Similarly, since migration of the terminal acetylene ligand from Os into its parallel bridging position to give dimetallacyclobutene resembles terminal-bridge CO rearrangement, the same triad dependence may be at play here as well. In addition, it is interesting to speculate on the probable influence of the "second metal" on this rearrangement step. It seems reasonable to suggest that, in view of the greater basicity of $Os(CO)_5$, the Os−acetylene bond is stronger in the $(CO)_5Os\rightarrow Os(CO)_3(C_2H_2)$ donor−acceptor species than in the $Ru(CO)_5$ analogue. Consequently, migration of the acetylene is more difficult in the Os−Os combination and contributes also to the smaller k_3 value. This may be taken as another example of metal−metal cooperativity in bimetallic systems.[25]

Formation of dimetallacyclopentenones **3** and **4** could proceed by direct attack of the terminal acetylene on a carbonyl ligand of the adjacent metal in intermediate **6** or by CO insertion in the dimetallacyclobutene formed from **6**, as depicted in Scheme 2. The former process was the mode favored by Casey et al.[26] for the formation of dimetallacyclopentenones, although intermediacy of dimetallacyclobutene could not be excluded. There are established precedents for the two-step process in Scheme 2. Puddephatt et al.[14] showed that $Ru_2(CO)_4(\mu\text{-dppm})_2(\mu\text{-}C_2H_2)$ undergoes CO insertion slowly at room temperature to give $Ru_2(CO)_4(\mu\text{-dppm})_2(\mu\text{-HCCHCO})$ (**5**). In our laboratories, Hoffman[27] has observed rapid PMe_3-promoted insertion of CO into $MRu(CO)_8(\mu\text{-}\eta^1,\eta^1\text{-}CF_3CCH)$ (M = Ru, Os) at room temperature, producing the dimetallacyclopentenones $MRu(CO)_8(\mu\text{-}\eta^1,\eta^1\text{-}CF_3CHCO)$, with insertion exclusively at the Ru-*C*H end of the molecule. Although no intermediates could be detected in the ^{13}C NMR-monitored reaction of $Os(CO)_4(\eta^2\text{-}C_2H_2)$ and $Ru(CO)_5$, the formation of the diosmacyclobutene **2** and the precedented CO insertion into the Ru−CH bond of dimetallacyclobutenes strongly support the process depicted in Scheme 2 for the formation of **3** and **4**. The lack of further reaction of **2** can be ascribed to the stronger Os−CH bond, which negates CO insertion.

The mechanism of the CO insertion step in the reaction with $Ru(CO)_5$ has been assumed to be analogous to that of $CH_3Mn(CO)_5$.[28] The latter is thought to occur by a solvent-assisted methyl migration followed by attack of the entering nucleophile on the unsaturated intermediate. However, in hydrocarbon solvents a path involving direct attack of the nucleophile has been suggested to be important.[29] We observe no apparent increase in rate in pentane saturated with CO, but rather that this gives saturation behavior with the rate being independent of [CO]. This is in contrast to the $CH_3Mn(CO)_5$ system, in which the rate is first-order in [CO] at ambient pressures of CO and saturation is achieved only at ∼15 atm of CO. The negative ΔS^* for the migration or insertion step, k_4, found here is in line with the previous observations[30] on $CH_3Mn(CO)_5$. For the $Ru(CO)_5$ system, the direct nucleophilic pathway for insertion is expected to be attenuated because the unsaturated intermediate in Scheme 2 is stabilized by coordination of the double bond of the dimetallacyclpentenone ring,[26,33] as illustrated in intermediate **A** in Scheme 2. The ability of the "HCCHCO" unit to act as a four-electron donor ligand provides built-in assistance for the CO insertion.[34] The weaker Ru−CH bond and more electrophilic Ru−CO ligand may conspire to give the much faster rate of insertion[35] in the present case, compared to the $Ru_2(CO)_4(\mu\text{-dppm})_2(\mu\text{-}\eta^1,\eta^1\text{-}C_2H_2)$ compound studied by Puddephatt et al.[14]

Finally, the observations with ^{13}CO-enriched $Ru(CO)_5$ and $Os(CO)_4(\eta^2\text{-}C_2H_2)$ should be discussed. The general scrambling of labels in the final product that is observed under benchtop conditions, with ^{13}CO in either reactant, can be ascribed to intermediate **6** undergoing carbonyl scrambling via **6′** along with the reversibility of the steps leading to its formation in Scheme 1. The most unusual observation from these experiments is that, in compound **3**, the CO on Ru trans to the acyl group derives exclusively from $Os(CO)_4(\eta^2\text{-}C_2H_2)$. The simplest explanation for this is to assume that this is the CO that is initially dissociated in Scheme 1 and added back in the final step of Scheme 2. This implies that the CO addition to the unsaturated intermediate in Scheme 2 is very stereoselective. This may be explained by reference to the "stabilized intermediate" **A** for the insertion process in Scheme 2. The Ru center can be described as six-coordinate with approximately octahedral geometry. One of the faces is occupied by the three terminal CO ligands and the other face by the ketonic carbonyl, the coordinated double bond, and the Os atom of the Ru−Os bond. The addition of CO may be pictured as in reaction 10. The *CO enters at the least sterically encumbered face of the Ru opposite the coordinated double bond. Detachment of the double bond, accompanied by movement of the CO ligands, as indicated, will result in the entering *CO being trans to the ketonic CO group in the final product, as found.

(24) Brown, T. L.; Zhang, S. *Inorg. Chem.* **1995**, *34*, 1164, and references therein, especially 6 and 7.

(25) (a) Torkelson, J. R.; Antwi-Nsiak, F. H.; McDonald, R.; Cowie, M.; Pruis, J. G.; Jalkanem, K. J.; DeKrock, R. L. *J. Am. Chem. Soc.* **1999**, *121*, 3683. (b) Sternberg, B. T.; Hilts, R. W.; Moro, G.; McDonald, R.; Cowie, M. *J. Am. Chem. Soc.* **1995**, *117*, 245.

(26) (a) Casey, C. P.; Cariño, R. S.; Sakaba, H. *Organometallics* **1997**, *16*, 419. (b) Casey, C. P.; Cariño, R. S.; Sakaba, H.; Hayashi, R. K. *Organometallics* **1996**, *15*, 2640. The observation are for the reaction of alkynes with $(C_5Me_5)(CO)_2Re{\equiv}Re(CO)_2(C_5Me_5)$ to form dimetallacyclopentenones, $(C_5Me_5)(CO)_2Re(\mu\text{-}\eta^1,\eta^3\text{-}CRCR'CO)Re(CO)(C_5Me_5)$.

(27) Hoffman, K. C. M.Sc. University of Alberta, 1994.

(28) Boese, W. T.; Ford, P. C. *J. Am. Chem. Soc.* **1995**, *117*, 8381, and references therein.

(29) Mawby, R. J.; Basolo, F.; Pearson, R. G. *J. Am. Chem. Soc.* **1964**, *86*, 3994.

(30) Calderazzo and Cotton[31] found that the reaction of CO with $CH_3Mn(CO)_5$ has $k_4k_5/k_{-4} = 8.99 \times 10^{-3}$ at 30 °C in (2,2′-diethoxy)-diethyl ether, with $\Delta H^* = 59.4$ kJ mol^{-1} and $\Delta S^* = -88.2$ J mol^{-1} K^{-1}, and Calderazzo[32] reported that $k_4 \approx 8 \times 10^{-4}$ under the same conditions. If $k_5/k_{-4} \leq 1$ and essentially temperature independent, then the ΔS^* for k_4 is even more negative than that for k_4k_5/k_{-4}.

(31) Calderazzo, F.; Cotton, F. A. *Inorg. Chem.* **1962**, *1*, 30.

(32) Calderazzo, F. *Angew. Chem., Int. Ed. Engl.* **1977**, *16*, 299.

(33) For other examples of dimetallacyclopentenone where the bridging unit functions as a four-electron donor, see the following and references therein: (a) Knox, S. A. R.; Lloyd, B. R.; Morton, D. A. V.; Orpen, A. G. Turner, M. L.; Hogarth, G. *Polyhedron* **1995**, *14*, 2723. (b) Kiel, G. Y.; Takats, J. *Organometallics* **1989**, *8*, 839.

(34) For an interesting metal-promoted CO insertion see: Collman, J. P.; Rothrock, R. K.; Finke, R. G.; Rose-Munch, F. *J. Am. Chem. Soc.* **1977**, *99*, 7381.

(35) For factors influencing migratory CO insertion see: Gonsalvi, L.; Adams, H.; Sunley, G. J.; Ditzel, E.; Haynes, A. *J. Am. Chem. Soc.* **1999**, *121*, 11233. (b) Axe, F. U.; Marynick, D. S. *J. Am. Chem. Soc.* **1988**, *110*, 3728.

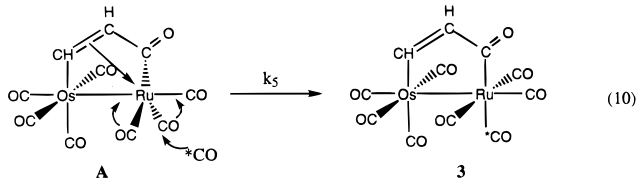

(10)

Experimental Section

General Procedures. All synthetic procedures and subsequent manipulations were carried out under purified argon or nitrogen atmospheres, using standard Schlenk techniques. Glassware was first heated in an oven at 160 °C to remove moisture and then cooled to room temperature either under vacuum or a stream of nitrogen, prior to use.

Materials. $RuCl_3{\cdot}nH_2O$ and OsO_4 were obtained from Johnson-Matthey Inc., acetylene and carbon monoxide were purchased from Matheson Gas Products Inc., and ^{13}CO and $^{13}C_2H_2$ were obtained from Isotec Inc. and Icon Services Inc., respectively. $Ru_3(CO)_{12}$[36a] and $Os_3(CO)_{12}$[36b] were prepared by published procedures or, for the latter, purchased from PGM Chemicals Ltd. The syntheses of $Os(CO)_5$[37a] and $Ru(CO)_5$[37b] also followed literature methods with the slight modifications reported recently.[38] The amount of $Os(CO)_5$ used in subsequent preparations was estimated from an "in-house" calibration curve of concentration (mg/mL) versus absorbance, while that of $Ru(CO)_5$ was calculated from the mass of $Ru_3(CO)_{12}$ used to prepare it. Pentane was pretreated sequentially with concentrated sulfuric acid, aqueous sodium bicarbonate, and distilled water before being dried over sodium sulfate and distilled from calcium hydride.

Instrumentation. The infrared spectra were recorded on Boemem MB-100 or Nicolet MX-1 FT spectrometers, over the range 2200−1600 cm^{-1}. The NMR spectra were recorded on Bruker WP-400, WM-360, or WM-200 MHz spectrometers. Chemical shifts, δ ppm, are relative to TMS, using the chemical shifts of the solvent as a secondary reference. Elemental analyses were carried out by the Microanalytical Laboratory of the Department of Chemistry.

Preparation of $Os(CO)_4(\eta^2\text{-}C_2H_2)$, 1a. A 100 mL volume immersion well, fitted with a GWV (Glaswerk Vertheim, $\lambda \geq$ 370 nm) cutoff filter, was precooled to −60 °C under an argon purge. The immersion well was charged with 75 mL of a pentane solution of $Os(CO)_5$ (3.0 mg/mL, 225 mg, 0.68 mmol). The temperature of the solution was maintained at −60 °C with a Lauda Klein-Kryomat circulating bath. Acetylene was passed through a dry ice/acetone-cooled (−78 °C) trap to remove the acetone stabilizer and purged through the solution at an approximate rate of 1 bubble per second (mineral oil bubbler). After 5−10 min of acetylene purge, photolysis was initiated (Philips HPK 125 W high-pressure Hg vapor lamp) while maintaining a constant acetylene purge. The progress of the reaction was monitored by IR spectroscopy, the intensity ratio of the 2036 (s), 1994 (vs) ν_{CO} bands of $Os(CO)_5$ reversing to 2036 (vs), 1994 (s) of the product. No changes in the intensities of these bands were seen after 90 min, but the photolysis was continued for an additional 30 min in order to ensure complete reaction. The solution was transferred by cannula under argon to a precooled (−78 °C) flask, and the solvent was removed in vacuo at −78 °C, giving a cream-colored residue. The residue was sublimed (ca. 0 °C, 10^{-3} mmHg) onto a dry ice-cooled probe to give $Os(CO)_4(\eta^2\text{-}C_2H_2)$ as a white, waxy solid, which decomposes above 0 °C. Consequently, the product was isolated by washing the probe with cold (−78 °C) pentane and collecting the colorless, thermally sensitive $Os(CO)_4(\eta^2\text{-}C_2H_2)$ solution in a precooled (−78 °C) flask. A yield of 82% (40 mL of 4.6 mg/mL, 184 mg, 0.56 mmol) was obtained. Due to its thermal instability, the product was characterized by spectroscopic means; no elemental analysis is available. The preparation has been performed numerous times and with various amounts of $Os(CO)_5$ (100−400 mg) with yields ranging from 60% to virtually quantitative (in experienced hands); ca. 200 mg of $Os(CO)_5$ and 2 h of photolysis are the recommended conditions. The concentration of **1a** (mg/mL), and thereby the yield, was estimated from a "titration" reaction with $Os(CO)_5$. As described below, this reaction gives octacarbonyldiosmacyclobutane, $Os_2(CO)_8(\mu\text{-}\eta^1,\eta^1\text{-}C_2H_2)$ (**2**), cleanly and virtually quantitatively (IR spectroscopy). IR (pentane, 10 °C, cm^{-1}): ν_{CO} 2121 (w), 2035 (vs), 2027 (m), 1996 (s); ν_{CC} 1642 (w). ^1H NMR (400 MHz, CD_2Cl_2, −83 °C): 6.16 (s, C_2H_2). $^{13}C\{^1H\}$ NMR (100.6 MHz, CD_2Cl_2, −86 °C): 73.5 (C_2H_2).

Preparation of $Os(CO)_4(\eta^2\text{-}C_2D_2)$. The C_2D_2 was generated from CaC_2 and D_2O. The procedure and workup were as described above. IR (pentane, 10 °C, cm^{-1}): ν_{CO} 2120 (w), 2035 (vs), 2027 (m), 1996 (s); ν_{CC} 1539 (w). ^2H NMR (61.4 MHz, CH_2Cl_2, −80 °C): 6.19 (br s, C_2D_2).

Preparation of $Os(CO)_4(\eta^2\text{-}^{13}C_2H_2)$. The same procedure was used, except that the photolysis was done under 1 atm of $^{13}C_2H_2$. The product was obtained in 41% yield. IR (pentane, 10 °C, cm^{-1}): ν_{CO} 2120 (w), 2035 (vs), 2026 (m), 1996 (s); ν_{CC} 1565 (w). ^{13}C NMR (100.6 MHz, CD_2Cl_2, −86 °C): 73.5 (AA′XX′: $^1J_{C-C}$ 92, $^1J_{C-H}$ 224, $^2J_{C-H}$ 20 Hz, C_2H_2).

Preparation of $Os(^{13}CO)_4(\eta^2\text{-}C_2H_2)$. The ^{13}CO enrichment was achieved by submitting a pentane solution of **1a** to three freeze−thaw degassing cycles and then stirring the solution at 0−10 °C for 2 h under 1 atm of ^{13}CO. To achieve a high level of enrichment, a second cycle of ^{13}CO was occasionally carried out. The pure product was isolated by low-temperature sublimation as described for **1a**. IR (pentane, 10 °C, cm^{-1}): ν_{CO} 2070 (w), 1991 (vs), 1980 (m), 1950 (s); ν_{CC} 1642 (w). $^{13}C\{^1H\}$ NMR (100.6 MHz, CD_2Cl_2, −82 °C): 179.9 (CO_{eq}), 173.3 (CO_{ax}), 73.5(C_2H_2).

Preparation of $Ru(CO)_4(\eta^2\text{-}C_2H_2)$, 1b. Utilizing the same setup and experimental conditions as for **1a**, a pentane solution of $Ru(CO)_5$ (generated from 73 mg of $Ru_3(CO)_{12}$ in 100 mL of pentane) was photolyzed at −60 °C for 2 h. The solvent was removed in vacuo at −78 °C, with exclusion of light. The resulting yellow, oily residue was sublimed at −20 °C onto a dry ice-cooled probe to give $Ru(CO)_4(\eta^2\text{-}C_2H_2)$ as an off-white, waxy solid, which decomposes at −10 °C: estimated yield ca. 80%, based on subsequent reaction with $Ru(CO)_5$. Due to its delicate nature, no elemental analysis is available. The ^{13}CO-enriched material, $Ru(^{13}CO)_4(\eta^2\text{-}C_2H_2)$, was prepared in the same way by starting with $Ru(^{13}CO)_5$. IR (pentane, −60 °C, cm^{-1}): ν_{CO} 2115 (w), 2037 (s), 2028 (m), 2002(s); ν_{CC} 1670 (w). ^1H NMR (400 MHz, CD_2Cl_2, −83 °C): 5.70 (s, C_2H_2). $^{13}C\{^1H\}$ NMR (100.6 MHz, CD_2Cl_2, −108 °C): 200.5 (CO_{eq}), 193.4 (CO_{ax}), 70.1 (C_2H_2).

Preparation of $Os_2(CO)_8(\mu\text{-}\eta^1,\eta^1\text{-}HCCH)$, 2. A cold (−78 °C) pentane solution (50 mL) of **1a** (50 mg, 0.152 mmol) and $Os(CO)_5$ (53 mg, 0.161 mmol) was slowly allowed to warm to 10 °C, and the solution was stirred at this temperature for 1 h. The progress of the reaction can be followed by IR spectroscopy, monitoring the growth of the 2082 cm^{-1} band of the product. The solution was concentrated in vacuo to about half of its volume and filtered (if necessary), and crystallization overnight at −80 °C afforded **2** as a moderately stable colorless to pale yellow solid, mp 76 °C (dec) (84.4 mg, 0.134 mmol, 88% yield). The various isotopomers were obtained using the same experimental procedures and appropriate starting materials as described for **1a**. IR (pentane, 25 °C, cm^{-1}): ν_{CO} 2129 (w), 2082 (s), 2042 (vs), 2024 (s), 2013 (s), 1997 (s). $^1H/^2H$ NMR (400/61.4 MHz, CD_2Cl_2/CH_2Cl_2, 25 °C): 6.96 (s, C_2H_2), 6.98 (br s, C_2D_2). $^{13}C\{^1H\}$ NMR (100.6 MHz, CD_2Cl_2, −86 °C): 178.4

(36) (a) Bruce, M. I.; Jensen, C. M.; Jones, N. L. *Inorg. Synth*. **1989**, *26*, 259. (b) Johnson, B. F. G.; Lewis, J.; Killy, P. A. *J. Chem. Soc. A* **1968**, 2859.

(37) (a) Rushman, P.; van Buuron, G. N.; Shiraliam, M.; Pomeroy, R. K. *Organometallics* **1983**, *2*, 693. (b) Johnson, B. F. G.; Lewis, J.; Twiggs, M. V. *J. Organomet. Chem*. **1974**, *67*, C75.

(38) Washington, J.; McDonald, R.; Takats, J.; Menashe, N.; Reshef, D.; Shvo, Y. *Organometallics* **1995**, *14*, 3996.

(2 CO_e), 173.9 (1 CO_u), 169.2 (1 CO_a), 98.4 (C_2H_2, coupled spectrum $^1J_{C-H}$ 156 Hz); from $Os_2(CO)_8(^{13}C_2H_2)$. ^{13}C NMR (100.6 MHz, CD_2Cl_2, −80 °C): 98.25 (AA′XX′; $^1J_{C-C}$ 57.2, $^1J_{C-H}$ 157.8, $^2J_{C-H}$ 0.4, $^3J_{H-H}$ 5.2 Hz C_2H_2). MS (70 eV, 120 °C): M^+, $M^+ - nCO$ ($n = 1-8$). Anal. Calcd for $C_{10}H_2O_8Os_2$: C, 19.05; H, 0.32. Found: C, 19.57; H, 0.47.

Preparation of $OsRu(CO)_8(\mu\text{-}\eta^1,\eta^1\text{-HCCHC(O)})$, 3. Cold (−78 °C) pentane solutions of **1a** (33.0 mL, 2.8 mg/mL, 92.4 mg, 0.282 mmol) and $Ru(CO)_5$ (generated from 59.0 mg of $Ru_3(CO)_{12}$ in 50 mL of pentane; 0.277 mmol of $Ru(CO)_5$) were mixed, and the colorless solution was slowly allowed to warm to ca. 8 °C and stirred at this temperature for 30 min; at this point, the color of the solution was pale yellow. The progress of the reaction can be followed by monitoring the disappearance of reactants at 2001 and 1997 cm^{-1} and formation of product at 2088 and 2047 cm^{-1}. The solvent was removed in vacuo (bath temperature ca. 5 °C). Crystallization of the residue from CH_2Cl_2/pentane at −80 °C afforded **3** as a moderately air-stable, yellow solid, mp 82 °C (dec) (150 mg, 0.262 mmol, 95% yield). The various isotopomers were obtained using the same experimental procedures and appropriate starting materials as described for **1a**. IR (pentane, 25 °C, cm^{-1}): ν_{CO} 2129 (w), 2126 (w), 2088 (s), 2055 (m), 2047 (vs), 2040 (s), 2019 (m), 2011 (s), 2000 (w); $\nu_{C=O}$ 1635 (m). ^1H NMR (400 MHz, CD_2Cl_2, 25 °C): 8.17 (d, J_{HH} 9 Hz, H_β), 7.46 (d, J_{HH} 9 Hz, H_α); ^2H NMR (61.4 MHz, CH_2Cl_2, 25 °C) 8.22 (br s, D_β), 7.48 (br s, D_α). ^{13}C NMR (100.6 MHz, CD_2Cl_2, 25 °C): 166.5 (d, J_{CH} 155 Hz, C_α), 131.4 (d, J_{CH} 150 Hz, C_β). $OsRu(^{13}CO)_8(\mu\text{-}C_2H_2{}^{13}CO)$ ^1H NMR (400 MHz, CD_2Cl_2, −86 °C): 8.17 (dq, $J_{HH} = J_{H\beta-C=O} = J_{H\beta-COu} = 9.2$, $J_{H\beta-COa} = 2.2$ Hz, H_β), 7.46 (dd, J_{HH} 9.2, $J_{H\alpha-C=O}$ 3.9 Hz, H_α). $^{13}C\{^1H\}$ NMR (100.6 MHz, CD_2Cl_2, −86 °C): 236.3 (d, $J_{C=O-COu}$ 18 Hz, Ru*C*═O),198.9 (s, 2 CO, RuCO_e), 190.9 (d, 1 CO, $J_{COu-C=O}$ 18 Hz, RuCO_u), 183.4 (s, 1 CO, RuCO_a), 182.9 (s, 2 CO, OsCO_e), 173.2 (s, 1 CO, OsCO_u), 165.5 (s, 1 CO, OsCO_a). $OsRu(^{13}CO)_8(\mu\text{-}^{13}C_2H_2{}^{13}CO)$ ^1H NMR (400 MHz, CD_3CN, −40 °C): 8.23 (br dq, J_{CH} 149, J_{HH} 9, $J_{H\beta-C=O}$ 9 Hz, H_β), 7.36 (br dd, J_{CH} 155, J_{HH} 9, $J_{H-C=O}$ 4.5 Hz, H_α). $^{13}C\{^1H\}$ NMR (100.6 MHz, CD_3CN, −40 °C): 237.8 (br d, $J_{C=Ou-CO\alpha}$ 39 Hz, Ru*C*═O), 200.9 (s, 2 CO, RuCO_e), 192.2 (d, $J_{COu-C=O}$ 15 Hz, RuCO_u), 186.0 (s, 1 CO, RuCO_a), 185.0 (s, 2 CO, OsCO_e), 175.0 (d, 1 CO, $J_{COu-C\beta}$ 15 Hz, OsCO_u), 167.2 (s, 1 CO, OsCO_a), 165.4 (dd, J_{CC} 62, $J_{C\alpha-C=O}$ 39 Hz, C_α), 135.2 (br d, J_{CC} 61 Hz, C_β). Anal. Calcd for $C_{11}H_2O_9OsRu$: C, 23.20; H, 0.35; O, 25.29. Found: C, 23.13; H, 0.41; O, 25.07.

Preparation of $Ru_2(CO)_8(\mu\text{-}\eta^1,\eta^1\text{-HCCHC(O)})$, 4. A cold (−78 °C) pentane solution containing **1b** and $Ru(CO)_5$ (each prepared from 73 mg, 0.114 mmol of $Ru_3(CO)_{12}$) was slowly allowed to warm to 10 °C and stirred at this temperature for 30 min. The solvent was removed in vacuo at 0 °C, and the residue was crystallized from CH_2Cl_2/pentane at −80 °C to give **4** as an orange solid of limited thermal stability at room temperature. The ^{13}CO-enriched material was prepared from $Ru(^{13}CO)_4(\eta^2\text{-}C_2H_2)$ and $Ru(^{13}CO)_5$. IR (pentane, 25 °C, cm^{-1}): ν_{CO} 2126 (w), 2086 (s), 2056 (m), 2048 (s), 2039 (s), 2028 (m), 2022 (m), 2012 (m); $\nu_{C=O}$ 1635 (m). ^1H NMR (400 MHz, CD_2Cl_2, 25 °C): 7.72 (d, J_{HH} 9 Hz, H_β), 6.87 (d, J_{HH} 9 Hz, H_α). ^{13}C NMR of ^{13}CO-enriched material (100.6 MHz, CD_2Cl_2, −80 °C): 235.6 (s, *C*═O), 201.1 (s, 2 $CO_{e'/e}$), 200.0 (s, 2 $CO_{e/e'}$), 191.6 (s, 2 $CO_{u/u'}$), 185.2 (s, 1 $CO_{a/a'}$), 184.7 (s, 1 $CO_{a'/a}$).

Attempted Reactions To Produce Other Bimetallic Products. Under the same experimental conditions as for the preparation of **3**, but instead of reacting $Ru(CO)_5$ with $Os(CO)_4(\eta^2\text{-}C_2H_2)$, the reverse reaction, addition of $Os(CO)_5$ to $Ru(CO)_4(\eta^2\text{-}C_2H_2)$, was carried out in an attempt to prepare **3**, or perhaps its regioisomer. No heterobimetallic product formed; only decomposition of $Ru(CO)_4(\eta^2\text{-}C_2H_2)$ was observed.

Similarly, attempts were made to produce FeM (M = Os, Ru) heterobimetallic products by reacting $Fe(CO)_5$ with $M(CO)_4(\eta^2\text{-}C_2H_2)$; again no heterobimetallic products were obtained.

Kinetic Methods. All solution transfers were done with gastight syringes. Stock solutions of $Os(CO)_4(\eta^2\text{-}C_2H_2)$ and $M(CO)_5$ in pentane were prepared in volumetric flasks that had been sealed with serum caps and purged with dry nitrogen. An appropriate volume of solvent was added by syringe, and the flasks were placed in a dry ice−acetone bath. An appropriate volume of a stock solution of $Os(CO)_4(\eta^2\text{-}C_2H_2)$ was added to the solution of $M(CO)_5$, and a sample of this solution was transferred to the infrared cell.

For reactions in which CO was added, the solution containing all reactants at dry ice temperature was purged with CO for 10−15 min before a sample was transferred to the infrared cell. The CO was purified of traces of $Fe(CO)_5$ by passing the gas through two hexane-filled gas scrubbers in dry ice/acetone baths and then through a liquid nitrogen−pentane trap to remove any hexane.

In all cases, the infrared cell was preequilibrated at the desired temperature for 30 min before use. A blank spectrum of the solvent, pentane, was recorded before each run. Temperature was maintained with a liquid circulating system described previously,[2] and the temperature of the cell was continuously monitored with a copper−constantan thermocouple. The infrared cell (Graseby Specac) was a gastight model with CaF_2 windows, amalgamated foil spacer and gaskets, a stainless steal body, and a 0.0475 cm path length.

The infrared spectra were recorded on a Boemem MB 100 spectrometer controlled by the software package Spectra-Calc running on an IBM-386 type computer. Spectra typically were recorded at equal time intervals over a range 1600−2300 cm^{-1}. Locally developed software was used to extract the absorbance at wavenumbers of interest for subsequent analysis on an IBM-486 type computer. The numerical integration program uses a fourth-order Runge−Kutta procedure. The fitting allows the delay time between mixing and the start of observation to be varied, and this was typically 3−4 min, as expected for transfer to the cell and temperature equilibration after handling.

Acknowledgment. We thank the Natural Sciences and Engineering Research Council of Canada for financial support for this work under the Cooperative Grants Program, and Dr. J. Washington for studies on the spontaneous decomposition of $Os(CO)_4(\eta^2\text{-}C_2H_2)$.

OM0000515